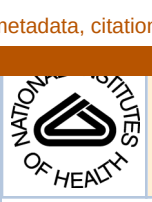

Published in final edited form as:

Curr Opin Chem Biol. 2011 April ; 15(2): 276–283. doi:10.1016/j.cbpa.2010.11.005.

A role for nickel-iron cofactors in biological carbon monoxide and carbon dioxide utilization

Yan Kung[1] and **Catherine L. Drennan**[1,2,3]

[1] Department of Chemistry, Massachusetts Institute of Technology, 77 Massachusetts Avenue, Cambridge, MA 02139

[2] Department of Biology, Massachusetts Institute of Technology, 77 Massachusetts Avenue, Cambridge, MA 02139

[3] Howard Hughes Medical Institute, Massachusetts Institute of Technology, 77 Massachusetts Avenue, Cambridge, MA 02139

Abstract

Ni-Fe containing enzymes are involved in the biological utilization of carbon monoxide, carbon dioxide, and hydrogen. Interest in these enzymes has increased in recent years due to hydrogen fuel initiatives and concerns over development of new methods for CO_2 sequestration. One Ni-Fe enzyme called carbon monoxide dehydrogenase (CODH) is a key player in the global carbon cycle and carries out the interconversion of the environmental pollutant CO and the greenhouse gas CO_2. The Ni-Fe center responsible for this important chemistry, the C-cluster, has been the source of much controversy, but several recent structural studies have helped to direct the field toward a unifying mechanism. Here we summarize the current state of understanding of this fascinating metallocluster.

While enzymes that utilize iron-containing active sites catalyze a wide range of well-known chemical transformations, three remarkable enzymes combine iron and nickel into complex metalloclusters that extend Nature's biochemical toolkit and lie at the heart of fundamental biological processes involving microbial hydrogen utilization and carbon fixation. [NiFe]-hydrogenase can catalyze both H_2 oxidation and evolution in anaerobic microbes to consume or produce protons and electrons, the biological equivalent of the hydrogen fuel cell anode [1,2]. Involved in carbon fixation, the enzyme acetyl-CoA synthase (ACS) contains a Ni-Fe-S active site metal center called the A-cluster that combines carbon monoxide (CO) with a methyl group and coenzyme A (CoA) to form acetyl-CoA, generating a source of carbon and energy for a variety of microbes. CO is often provided to ACS by another Ni-Fe enzyme called carbon monoxide dehydrogenase (CODH), a dimeric enzyme which contains a distinctive Ni-Fe-S metal center termed the C-cluster that carries out the reversible reduction of carbon dioxide (CO_2) to CO, the biological equivalent of the water-gas shift reaction and a mechanism for CO_2 utilization. Interest in all three enzymes has increased dramatically in recent years due to renewed attention in the development of hydrogen fuel cells and the design of CO_2 sequestration technologies. While the first X-ray crystal structures of [NiFe]-hydrogenase [3], ACS [4], and CODH [5,6] revealed the overall

---

Corresponding author: Drennan, C.L. (cdrennan@mit.edu, Tel: 617-253-5622, Fax: 617-258-7847).

architecture of these complex metallocenters, recent work has aimed to develop an understanding of the mechanisms by which these clusters catalyze their respective reactions. As major advances have been made on the C-cluster within the last three years, we have focused this review on this metallocenter. Although the CODH literature has had its share of controversies, the CODH community is now converging on a consensus mechanism, a timely achievement toward understanding one of nature's solutions for CO_2 utilization.

CODH and the global carbon cycle

CODH plays a central role in the global carbon cycle in anaerobic microorganisms (Figure 1). Some microbes, such as *Rhodospirillum rubrum* and *Carboxydothermus hydrogenoformans* depend upon a monofunctional CODH in their ability to use CO oxidation as a sole carbon and energy source [7,8]. It is estimated that CODH activity accounts for the annual removal of ~10^8 tons of CO from the environment [9]. Acetogenic bacteria, such as *Moorella thermoacetica*, couple CODH-catalyzed reduction of CO_2 to CO with synthesis of acetyl-CoA in a bifunctional CODH/ACS complex [10]. Here, CO produced from CO_2 at the C-cluster is a gaseous intermediate that travels approximately 70 Å through an extraordinary hydrophobic tunnel within the enzyme complex [4,11–14] to the ACS A-cluster, where it becomes the carbonyl of acetyl-CoA. Acetyl-CoA is then either converted into cellular biomass, or its high energy thioester bond can be cleaved to drive phosphorylation of ADP to ATP in supplying energy for the cell, producing acetate as a waste product. It is estimated that ~10^{11} tons of acetate are produced globally from CO_2 through this process every year by anaerobic acetogens [15]. Additionally, CODH and ACS components are present in the acetyl-CoA decarbonylase/synthase (ACDS) complex, a multienzyme machine that is a major route to methane production in methanogenic archaea, which generate an estimated 10^9 tons of methane per year [16,17].

Initial structural and mechanistic studies of CODH

Although it had been well established that CODH harbored a Ni-Fe-S active site (see [18] for review), it was not until the initial X-ray crystal structures of CODH from *R. rubrum* (*Rr*CODH) (Figure 2A) [6], *C. hydrogenoformans* (*Ch*CODH) [5], and *M. thermoacetica* CODH/ACS (*Mt*CODH/ACS) (Figure 2B) [4,13] that the arrangement and geometry of the metals were determined. Early spectroscopic studies had suggested that the C-cluster was composed of a [4Fe-4S] cubane with a unique Ni site nearby [18,19]. However, all of these CODH structures revealed an unprecedented metallocluster that can be described as a distorted [Ni-3Fe-4S] cubane coordinated to a unique Fe site, also called ferrous component II (FCII).

Despite exhibiting the same arrangement of metals in the C-cluster, these initial structures possessed key differences that hindered full mechanistic understanding. Perhaps most importantly, the *Ch*CODH C-cluster contained an additional sulfide ligand in a position bridging Ni of the distorted cubane and the unique Fe (Figure 2C), a feature absent in the *Rr*CODH and *Mt*CODH/ACS structures (Figure 2D). This inconsistency led to controversy over the correct composition of the cluster, and further experiments were conducted which argued either for [20] or against [21,22] a catalytic role for the sulfide bridge.

Related to the issue of the sulfide bridge is the crucial question of where substrates bind to the C-cluster for the interconversion of CO and CO_2. In the direction of CO oxidation, CO and H_2O must bind the C-cluster, H_2O is deprotonated, and CO_2 is formed, generating two protons and two electrons that reduce the cluster. Although the pathway by which protons exchange with the bulk solvent is not firmly established, a network of histidine residues that link the buried C-cluster with the solvent exterior has been suggested as a possible route [6,23]. Electrons are passed from the C-cluster to the surface of the protein through

additional [4Fe-4S] clusters that form a wire seen in all CODH structures (Figure 2A). Ferredoxin, pyruvate:ferredoxin oxidoreductase (PFOR), and hydrogenase have been proposed as ultimate electron acceptors [24,25]; intermolecular electron transfer has been suggested to be rate-limiting [26], with specific activity depending upon the electron acceptor employed [27,28]. In the direction of CO_2 reduction, CO_2 must bind the two-electron reduced C-cluster [29,30], and with the addition of two protons, H_2O and CO are formed.

While there remained uncertainties surrounding the transfer of electrons and protons to the buried C-cluster, the most attention has been paid to binding sites for CO and H_2O on the metals of the C-cluster. Studies conducted prior to the *Ch*CODH and *Rr*CODH structure determinations had indicated that Ni and Fe are involved in binding the substrate CO and water molecules, respectively [19,31]. In the *Ch*CODH structure, however, the sulfide bridge fills coordination sites to complete square planar geometry around Ni and distorted tetrahedral geometry around the unique Fe, making the substrate binding locations unclear. Although *Rr*CODH and two independent *Mt*CODH/ACS structures contain empty coordination sites in place of the sulfide bridge, electron density for an unassigned ligand apical to Ni was present in the *Rr*CODH structure and one *Mt*CODH/ACS structure [6,13]. Without a clear identification of substrate binding sites, the mechanism of the C-cluster remained enigmatic.

Substrate- and inhibitor-bound C-cluster structures identify the active site

Over the past three years, many crystal structures have been solved that depict substrates bound to the C-cluster. Structures of *Ch*CODH [32] and *Mt*CODH/ACS [33] show the substrate water molecule bound to the unique Fe site in an identical fashion, completing a distorted tetrahedral geometry (Figure 3A). These observations are consistent with previous studies which also suggest that water binds Fe [31]. None of these structures contain the sulfide bridge, as the water molecule occupies the sulfide coordination site on Fe.

A structure of the CODH component of the ACDS complex from *Methanosarcina barkeri* (*Mb*CODH) depicts CO bound to Ni of the C-cluster in a position adjacent the water molecule, which remains bound to the unique Fe (Figure 3B) [34]. With both substrates bound to the cluster, it was hypothesized that the low pH of the crystallization condition (4.6) prevented turnover by disfavoring deprotonation of water to the active hydroxide nucleophile, allowing the capture of the C-cluster state immediately before catalysis. CO is bound to Ni in an unexpected bent conformation, with a Ni-C-O bond angle of 103°, completing a distorted tetrahedral geometry. Interestingly, a structure of cyanide, a CODH inhibitor, bound to the *Mt*CODH/ACS C-cluster illustrates analogous bent geometry (Figure 3B), with a Ni-C-N bond angle of ~114° [33]. The substrate water molecule in this structure also remains bound to the unique Fe. A conserved isoleucine residue is seen in both structures to sterically block linear binding of CO and cyanide to Ni (Figure 3B). Such bent coordination is not likely to be stable; indeed, infrared spectroscopy had suggested that there is no single, stable site for CO binding to the C-cluster [35]. Thus, it is possible that binding of CO to give bent geometry is mechanistically important, as the enhanced stability of a linear binding mode may impede turnover. In this model, isoleucine would contribute to ground state destabilization, lowering the activation barrier to catalysis by preventing linear substrate binding.

The structures of CO and cyanide bound to the C-cluster place the carbon atom and water molecule too far apart for catalysis; a shift in coordination must occur during the reaction. The crystal structure of the product CO_2 bound to the *Ch*CODH C-cluster [32] provides a unique perspective on how such a shift may occur. Here, the CO_2 carbon is bound to Ni,

while one CO_2 oxygen is bound to the unique Fe. A superposition of CO_2-bound *Ch*CODH with CO-bound *Mb*CODH and cyanide-bound *Mt*CODH/ACS structures exhibits a nearly identical position of all substrate atoms except for the carbon atom (Figure 3C). While the oxygen/nitrogen atoms remain stationary across the structures, the carbon atom has shifted closer to the water molecule in the CO_2-bound structure. This "carbon shift" has been proposed [33] to alter the Ni coordination geometry from distorted tetrahedral in the CO- and CN-bound forms to square planar in the CO_2-bound form.

Taken together, these structures reveal the active site on the C-cluster of CODH. In the direction of CO oxidation, crystal structures from *Ch*CODH, *Mb*CODH, and *Mt*CODH/ACS depict water bound to the unique Fe, while structures of *Mb*CODH and *Mt*CODH/ACS show CO or an inhibitor CN^- bound to Ni, respectively. Meanwhile, one structure of *Ch*CODH shows CO_2, the substrate in the direction of CO_2 reduction, bound to the cluster. In all structures, regardless of the organism, no sulfide bridge is present when a substrate molecule is bound. Consistent with these structures, a catalytic mechanism is proposed (Figure 4).

The complexity of cyanide inhibition

A distinguishing feature of all Ni-containing CODHs is potent inhibition by cyanide [24,27,36–40]. Although direct binding to the C-cluster has been implicated as the root of cyanide inhibition, years of study have not led to a clear inhibitory mechanism. On one hand, cyanide has been described as a competitive inhibitor that binds Ni: Ni-deficient *Rr*CODH does not bind cyanide [37,38], and X-ray absorption spectroscopy (XAS) indicated that cyanide shares with CO a binding site on Ni with a Ni-C distance of 1.81–1.84 Å [40]. In contrast, other studies have suggested that cyanide binds Fe: electron-nuclear double resonance (ENDOR) spectroscopy indicated that cyanide displaces the Fe-bound water molecule [31], and Mössbauer spectroscopy showed a change in quadrupole splitting (ΔE_Q) of the unique Fe signal upon cyanide treatment [19]. It has also been suggested that cyanide may bind at multiple sites [26].

However, these data appear to be in conflict only if it is assumed that cyanide must adopt a single binding mode. Indeed, two crystal structures of cyanide bound to the C-cluster show that the same inhibitor can actually adopt multiple binding modes. As mentioned above, the cyanide-bound *Mt*CODH/ACS structure [33] shows cyanide bound to Ni in a bent conformation, in an analogous fashion as CO in the *Mb*CODH structure, with water still bound to Fe (Figure 3B). The cyanide carbon completes distorted tetrahedral geometry around Ni and mimics how CO binds to the active C-cluster. On the other hand, a cyanide-bound *Ch*CODH structure [41] shows CN^- bound to Ni with effectively linear geometry (Ni-C-N bond angle of 175°), conferring square planar geometry around Ni. Notably, the substrate water molecule is absent in this structure, which represents an inhibited form where neither substrate is bound to the cluster. A superposition of the two cyanide-bound C-clusters is shown in Figure 3D.

These dissimilar crystal structures depicting cyanide binding mirror the seemingly contradictory spectroscopic results described above. It has been recently suggested that a rapid, reversible cyanide binding step is followed by a slow rearrangement step to achieve tighter binding [26,41], explaining how cyanide could be both a rapid, reversible inhibitor under some conditions as well as a slow-binding inhibitor under others [38]. Here, we reason that the *Mt*CODH/ACS cyanide structure illustrates an "easily reversible" cyanide binding mode, where cyanide binds Ni in the same bent manner as CO. This bent, Ni-bound cyanide structure is consistent with studies indicating that cyanide is a competitive inhibitor of CO and, like CO, binds Ni. In a subsequent, slow rearrangement step, the substrate water

molecule bound to the unique Fe may then be displaced, freeing space to allow cyanide to relax into a more favored linear binding mode, represented by the *Ch*CODH cyanide structure. One would expect this structure to represent cyanide in a “tight binding” mode. The displacement of the Fe-bound water molecule upon cyanide treatment seen in the *Ch*CODH structure is consistent with the ENDOR experiments [31] and further clarifies that water displacement is not a result of direct binding of cyanide to Fe, an assumption made in the ENDOR study. Water displacement and linear cyanide binding can also explain why Mössbauer spectroscopy showed a change in ΔE_Q of the unique Fe signal upon cyanide treatment [19]. Therefore, while neither cyanide-bound C-cluster structure can alone reconcile all of the spectroscopic studies, both structures together can provide an explanation for the seemingly inconsistent data on CODH cyanide inhibition, a twenty-year mystery in the field.

In asking why the *Ch*CODH and *Mt*CODH/ACS structures revealed different cyanide binding modes, the most likely answer lies in the dissimilar cyanide crystal soaking protocols. *Ch*CODH crystals were soaked for 30 min in 70 mM KCN [41], while *Mt*CODH/ACS crystals were soaked for 1 h in only 100 μM KCN [33]. Because *Ch*CODH crystals were exposed to cyanide concentrations a few orders of magnitude higher than *Mt*CODH/ACS crystals, it is possible that the equilibrium was shifted towards displacement of Fe-bound water bound and linear cyanide binding. Regardless, these structures have offered a clearer picture of the mechanism of cyanide inhibition (Figure 4).

Conclusions

The truly distinctive $NiFe_4S_4$ CODH C-cluster has inspired decades of biochemical research; however, the literature has been fraught with controversy and contradictions regarding the C-cluster’s structure, mechanism, and mode of inhibition. Crystal structures of CODHs from several organisms have brought the C-cluster into focus and allowed us to rationalize the abundance of seemingly inconsistent biochemical data. From these structural studies, a unified view of the C-cluster has emerged, presenting key insights into the function of this remarkable and environmentally important metallocluster.

Acknowledgments

Work in the Drennan laboratory on carbon monoxide dehydrogenase has been supported by the National Institutes of Health (GM69857) and the MIT Energy Initiative. C.L.D. is a Howard Hughes Medical Institute Investigator.

References

* - of special interest

** - of outstanding interest

1. Fontecilla-Camps JC, Volbeda A, Cavazza C, Nicolet Y. Structure/Function Relationships of [NiFe]- and [FeFe]-Hydrogenases. Chem Rev. 2007; 107:4273–4303. [PubMed: 17850165]
2. Vignais PM, Billoud B. Occurrence, Classification, and Biological Function of Hydrogenases: An Overview. Chem Rev. 2007; 107:4206–4272. [PubMed: 17927159]
3. Volbeda A, Charon M-H, Piras C, Hatchikian EC, Frey M, Fontecilla-Camps JC. Crystal structure of the nickel-iron hydrogenase from *Desulfovibrio gigas*. Nature. 1995; 373:580–587. [PubMed: 7854413]
4*. Doukov TI, Iverson TM, Seravalli J, Ragsdale SW, Drennan CL. A Ni-Fe-Cu center in a bifunctional carbon monoxide dehydrogenase/acetyl-CoA synthase. Science. 2002; 298:567–572. The crystal structure of *Mt*CODH/ACS (2.20 Å resolution) was first described in this paper. The

C-cluster here did not contain the μ_2-S ligand seen in the structure of *Ch*CODH that bridges Ni and the unique Fe. [PubMed: 12386327]

5*. Dobbek H, Svetlitchnyi V, Gremer L, Huber R, Meyer O. Crystal Structure of a Carbon Monoxide Dehydrogenase Reveals a [Ni-4Fe-5S] Cluster. Science. 2001; 293 The crystal structure of *Ch*CODH (1.63 Å resolution) was first shown and depicted a C-cluster similar to that of *Rr*CODH, except for the presence of a μ_2-S ligand bridging Ni and the unique Fe. Although no ligand apical to Ni was present, it was suggested that CO may bind to this site.

6*. Drennan CL, Heo J, Sintchak MD, Schreiter E, Ludden PW. Life on Carbon Monoxide: X-ray Structure of *Rhodospirillum rubrum* Ni-Fe-S Carbon Monoxide Dehydrogenase. Proc Natl Acad Sci USA. 2001; 98:11973–11978. This paper presented the 2.80 Å resolution crystal structure of *Rr*CODH, which is similar to that of *Ch*CODH but contains an unknown ligand apical to Ni of the C-cluster and lacks a μ_2-S ligand bridging Ni and the unique Fe. [PubMed: 11593006]

7. Uffen RL. Anaerobic growth of a *Rhodopseudomonas* species in the dark with carbon monoxide as sole carbon and energy substrate. Proc Natl Acad Sci US A. 1976; 73:3298–3302.

8. Svetlichny VA, Sokolova TG, Gerhardt M, Ringpfeil M, Kostrikina NA, Zavarzin GA. *Carboxydothermus hydrogenoformans* gen. nov., sp. nov., a CO-utilizing thermophilic anaerobic bacterium from hydrothermal environments of Kunashir Island. Syst Appl Microbiol. 1991; 14:254–260.

9. Bartholomew GW, Alexander M. Microbial Metabolism of Carbon Monoxide in Culture and in Soil. Appl Environ Microbiol. 1979; 37:932–937. [PubMed: 485139]

10. Ragsdale SW, Pierce E. Acetogenesis and the Wood-Ljungdahl Pathway of CO_2 fixation. Biochim Biophys Acta. 2008; 1784:1873–1898. [PubMed: 18801467]

11. Maynard EL, Lindahl PA. Evidence of a Molecular Tunnel Connecting the Active Sites for CO_2 Reduction and Acetyl-CoA Synthesis in Acetyl-CoA Synthase from *Clostridium thermoaceticum*. J Am Chem Soc. 1999; 121:9221–9222.

12. Seravalli J, Ragsdale SW. Channeling of Carbon Monoxide during Anaerobic Carbon Dioxide Formation. Biochemistry. 2000; 39:1274–1277. [PubMed: 10684606]

13. Darnault C, Volbeda A, Kim EJ, Legrand P, Vernede X, Lindahl PA, Fontecilla-Camps JC. Ni-Zn-[Fe4-S4] and Ni-Ni-[Fe4-S4] clusters in closed and open subunits of acetyl-CoA synthase/carbon monoxide dehydrogenase. Nat Struct Biol. 2003; 10:271–279. [PubMed: 12627225]

14*. Doukov TI, Blasiak LC, Seravalli J, Ragsdale SW, Drennan CL. Xenon in and at the end of the tunnel of bifunctional carbon monoxide dehydrogenase/acetyl-CoA synthase. Biochemistry. 2008; 47:3474–3483. This 2.51 Å resolution crystal structure of *Mt*CODH/ACS pressurized with xenon depicts how CO generated at the C-cluster from CO_2 reduction can make its way through a buried tunnel to the A-cluster for acetyl-CoA synthesis. [PubMed: 18293927]

15. Drake, HL.; Daniel, SL.; Matthies, C.; Küsel, K. Acetogenesis, acetogenic bacteria, and the acetyl-CoA pathway: past and current perspectives. In: Drake, HL., editor. Acetogenesis. Chapman and Hall; 1994. p. 3-60.

16. Grahame DA. Catalysis of Acetyl-CoA Cleavage and Tetrahydrosarcinapterin Methylation by a Carbon Monoxide Dehydrogenase-Corrinoid Enzyme Complex. J Biol Chem. 1991; 266:22227–22233. [PubMed: 1939246]

17. Thauer RK. Biochemistry of Methanogenesis: A Tribute to Marjory Stephenson. Microbiology. 1998; 144:2377–2406. [PubMed: 9782487]

18. Ragsdale SW, Kumar M. Nickel-Containing Carbon Monoxide Dehydrogenase/Acetyl-CoA Synthase. Chem Rev. 1996; 96:2515–2539. [PubMed: 11848835]

19. Hu Z, Spangler HJ, Andersen ME, Xia J, Ludden PW, Lindahl PA, Münck E. Nature of the C-Cluster in Ni-Containing Carbon Monoxide Dehydrogenases. J Am Chem Soc. 1996; 118:830–845.

20. Dobbek H, Svetlitchnyi V, Liss J, Meyer O. Carbon Monoxide Induced Decomposition of the Active Site [Ni-4Fe-5S] Cluster of CO Dehydrogenase. J Am Chem Soc. 2004; 126:5382–5387. [PubMed: 15113209]

21. Feng J, Lindahl PA. Effect of Sodium Sulfide on Ni-Containing Carbon Monoxide Dehydrogenases. J Am Chem Soc. 2004; 126:9094–9100. [PubMed: 15264843]

22. Gu W, Seravalli J, Ragsdale SW, Cramer SP. CO-Induced Structural Rearragement of the C Cluster in *Carboxydothermus hydrogenoformans* CO Dehydrogenase-Evidence from Ni K-Edge X-ray Absorption Spectroscopy. Biochemistry. 2004; 43:9029–2035. [PubMed: 15248760]

23. Kim EJ, Feng J, Bramlett MR, Lindahl PA. Evidence for a Proton Transfer Network and a Required Persulfide-Bond-Forming Cysteine Residue in Ni-Containing Carbon Monoxide Dehydrogenases. Biochemistry. 2004; 43:5728–5734. [PubMed: 15134447]

24. Ragsdale SW, Clark JE, Ljungdahl LG, Lundie LL, Drake HL. Properties of Purified Carbon Monoxide Dehydrogenase from *Clostridium thermoaceticum*, a Nickel, Iron-Sulfur Protein. J Biol Chem. 1983; 258:2364–2369. [PubMed: 6687389]

25. Menon S, Ragsdale SW. Unleashing Hydrogenase Activity in Carbon Monoxide Dehydrogenase/Acetyl-CoA Synthase and Pyruvate:Ferredoxin Oxidoreductase. Biochemistry. 1996; 35:15814–15821. [PubMed: 8961945]

26. Seravalli J, Ragsdale SW. ^{13}C NMR Characterization of an Exchange Reaction between CO and CO_2 Catalyzed by Carbon Monoxide Dehydrogenase. Biochemistry. 2008; 47:6770–6781. [PubMed: 18589895]

27. Andersen ME, DeRose VJ, Hoffman BM, Lindahl PA. Identification of a Cyanide Binding Site in CO Dehydrogenase from *Clostridium thermoaceticum* Using EPR and ENDOR Spectroscopies. J Am Chem Soc. 1993; 115:12204–12205.

28. Svetlitchnyi V, Peschel C, Acker G, Meyer O. Two Membrane-Associated NiFeS-Carbon Monoxide Dehydrogenases from the Anaerobic Carbon-Monoxide-Utilizing Eubacterium *Carboxydothermus hydrogenoformans*. J Bacteriol. 2001; 183:5134–5144. [PubMed: 11489867]

29. Andersen ME, Lindahl PA. Spectroscopic States of the CO Oxidation/CO_2 Reduction Active Site of Carbon Monoxide Dehydrogenase and Mechanistic Implications. Biochemistry. 1996; 35:8371–8390. [PubMed: 8679595]

30. Seravalli J, Kumar M, Lu W-P, Ragsdale SW. Mechanism of Carbon Monoxide Oxidation by the Carbon Monoxide Dehydrogenase/Acetyl-CoA Synthase from *Clostridium thermoaceticum*: Kinetic Characterization of the Intermediates. Biochemistry. 1997; 36:11241–11251. [PubMed: 9287167]

31. DeRose VJ, Telser J, Andersen ME, Lindahl PA, Hoffman BM. A Multinuclear ENDOR Study of the C-Cluster in CO Dehydrogenase from *Clostridium thermoaceticum*: Evidence for H_xO and Histidine Coordination to the $[Fe_4S_4]$ Center. J Am Chem Soc. 1998; 120:8767–8776.

32**. Jeoung J-H, Dobbek H. Carbon Dioxide Activation at the Ni, Fe-Cluster of Anaerobic Carbon Monoxide Dehydrogease. Science. 2007; 318:1461–1464. Three structures of *Ch*CODH presented here identified both the water and CO_2 binding sites of the C-cluster and provided the first images of substrates bound to the cluster. Water was bound in the same fashion to the unique Fe of the C-cluster in two structures (1.40 and 1.48 Å resolution) at differing redox states. The redox state was modulated by soaking crystals in solutions at different reduction potentials. CO_2 binding was observed in one structure (1.50 Å resolution) after soaking crystals in sodium bicarbonate. [PubMed: 18048691]

33**. Kung Y, Doukov TI, Seravalli J, Ragsdale SW, Drennan CL. Crystallographic Snapshots of Cyanide- and Water-Bound C-Clusters from Bifunctional Carbon Monoxide Dehydrogenase/Acetyl-CoA Synthase. Biochemistry. 2009; 48:7432–7440. Two crystal structures of *Mt*CODH/ACS were presented in this paper (both at 2.15 Å resolution). The first showed water bound to the unique Fe of the C-cluster in the same fashion as in the *Ch*CODH C-cluster. The second structure, obtained after crysals were soaked in 100 μM KCN for 1 h, illustrated water bound to the unique Fe and cyanide bound to Ni with bent geometry. [PubMed: 19583207]

34**. Gong W, Hao B, Wei Z, Ferguson DJJ, Tallant T, Krzycki JA, Chan MK. Structure of the $\alpha_2\varepsilon_2$ Ni-Dependent CO Dehydrogenase Component of the *Methanosarcina barkeri* acetyl-CoA decarbonylase/synthase complex. Proc Natl Acad Sci USA. 2008; 105:9558–9563. This paper described a 2.00 Å resolution crystal structure of *Mb*CODH with the substrate water molecule bound to the unique Fe of the C-cluster and CO bound to Ni with bent geometry. *Mb*CODH was proposed to have not turned over due to the acidic conditions of the crystallization condition. [PubMed: 18621675]

35. Chen J, Huang S, Seravalli J, Gutzma HJ, Swartz DJ, Ragsdale SW, Bagley KA. Infrared Studies of Carbon Monoxide Binding to Carbon Monoxide Dehydrogenase/Acetyl-CoA Synthase from *Moorella thermoacetica*. Biochemistry. 2003; 42:14822–14830. [PubMed: 14674756]

36. Grahame DA, Stadtman TC. Carbon Monoxide Dehydrogeanse from *Methanosarcina barkeri*: Disaggregation, Purification, and Physicochemical Properties of the Enzyme. J Biol Chem. 1987; 262:3706–3712. [PubMed: 3818661]

37. Ensign SA, Bonam D, Ludden PW. Nickel is Required for the Transfer of Electrons from Carbon Monoxide to the Iron-Sulfur Center(s) of Carbon Monoxide Dehydrogenase from *Rhodospirillum rubrum*. Biochemistry. 1989; 28:4968–4973. [PubMed: 2504284]

38. Ensign SA, Hyman MR, Ludden PW. Nickel-Specific, Slow-Binding Inhibition of Carbon Monoxide Dehydrogenase from *Rhodospirillum rubrum* by Cyanide. Biochemistry. 1989; 28:4973–4979. [PubMed: 2504285]

39. Andersen ME, Lindahl PA. Organization of Clusters and Internal Electron Pathways in CO Dehydrogenase from *Clostridium thermoaceticum*: Relevance to the Mechanism of Catalysis and Cyanide Inhibition. Biochemistry. 1994; 33:8702–8711. [PubMed: 8038160]

40. Ha S-W, Korbas K, Klepsch M, Meyer-Klaucke W, Meyer O, Svetlitchnyi V. Interaction of Potassium Cyanide with the [Ni-4Fe-5S] Active Site Cluster of CO Dehydrogenase from *Carboxydothermus hydrogenoformans*. J Biol Chem. 2007; 282:10639–10646. [PubMed: 17277357]

41**. Jeoung J-H, Dobbek H. Structural Basis of Cyanide Inhibition of Ni, Fe-Containing Carbon Monoxide Dehydrogenase. J Am Chem Soc. 2009; 131:9922–9923. This paper describes the 1.36 Å resolution crystal structure of *Ch*CODH with cyanide bound to Ni of the C-cluster with near-linear geometry. In this structure, obtained after crystals were soaked in 70 mM KCN for 30 min, the substrate water molecule is notably absent, unlike the structure of *Mt*CODH/ACS with both cyanide and water bound to the C-cluster. [PubMed: 19583208]

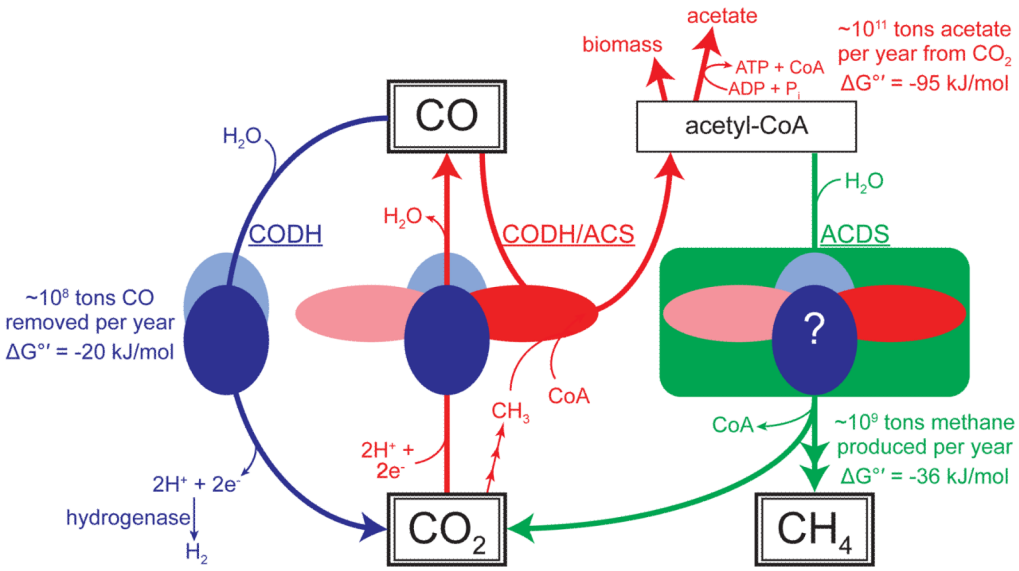

Figure 1.

Schematic of NiFe-containing CODH in the microbial carbon cycle and its contributions to CO, CO_2, and methane production and consumption. CODH is shown as a dimer in light and dark blue ovals, ACS as light and dark red ovals, and the methanogenic ACDS complex as a green rectangle containing both CODH and ACS components in an unknown arrangement.

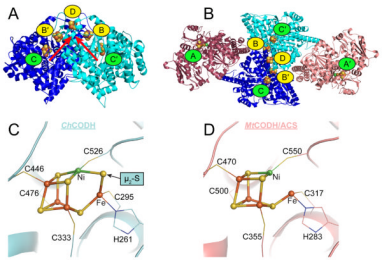

Figure 2.

CODH and C-cluster structures. **(A)** The *Rr*CODH homodimer (PDB ID: 1JQK) and **(B)** the bifunctional *Mt*CODH/ACS complex (PDB ID: 1MJG); CODH subunits in blue and cyan ribbons, and ACS subunits in dark and light pink ribbons. Metalloclusters in spheres: Ni in green, Cu in brown, Fe in orange, S in yellow. Active site A- and C-clusters are labelled in green and are $NiFe_4S_4$ and $Ni_2Fe_4S_4$ clusters, respectively. B- and D-clusters are labelled in yellow and are Fe_4S_4 cubanes involved in electron transfer, with red arrows in (A) indicating the direction of electron flow during CO oxidation. **(C)** The C-cluster of *Ch*CODH (PDB ID: 1SU8, cyan ribbons), which contains a sulfido ligand (labelled μ_2-S) that bridges Ni and the unique Fe. **(D)** The C-cluster of *Mt*CODH/ACS (pink ribbons), which does not contain the bridging sulfide. C-clusters in ball-and-stick: Ni in green, Fe in orange, and S in yellow. Protein ligands in sticks: N in blue, S in yellow, and C following protein ribbon coloring. Residue numberings follow the respective protein sequences.

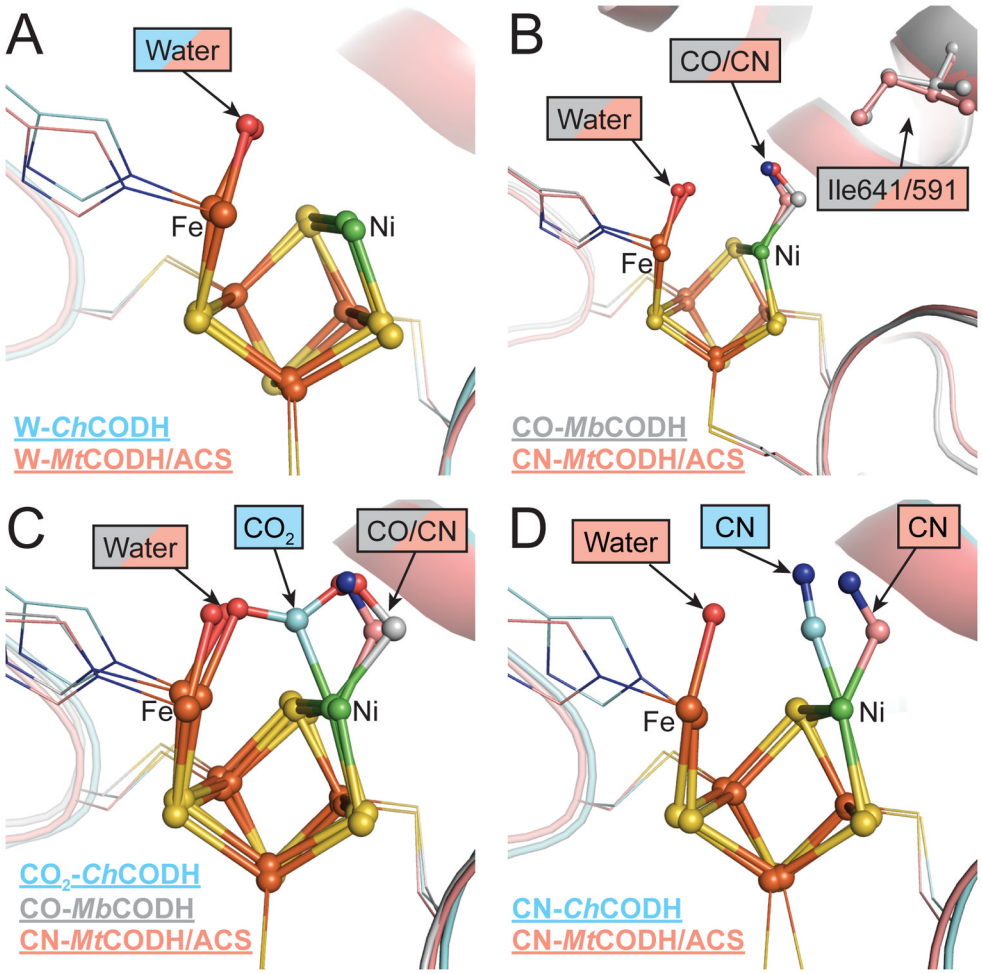

Figure 3.

Substrate and inhibitor bound C-cluster structures. **(A)** Superposition of water-bound C-clusters from *Ch*CODH and *Mt*CODH/ACS. **(B)** Superposition of CO/water- and cyanide/water-bound C-clusters from *Mb*CODH and *Mt*CODH/ACS, respectively. A conserved isoleucine residue (Ile641 in *Mb*CODH and Ile591 in *Mt*CODH/ACS) that is believed to sterically impede linear CO/CN-binding is shown in ball-and-stick. **(C)** Superposition of the structures in (B) plus the CO_2-bound C-cluster from *Ch*CODH. **(D)** Superposition of the cyanide-bound C-clusters from *Mt*CODH/ACS and *Ch*CODH. Protein chains in ribbons: *Ch*CODH in cyan, *Mt*CODH/ACS in pink, and *Mb*CODH in gray. C-clusters in ball-and-stick, and protein ligands to the cluster in sticks: Ni in green, Fe in orange, S in yellow, N in blue, O in red, and C following protein ribbon coloring. The Ni and unique Fe sites are labeled “Ni” and “Fe”, respectively. For clarity, not all protein ligands to the cluster are shown.

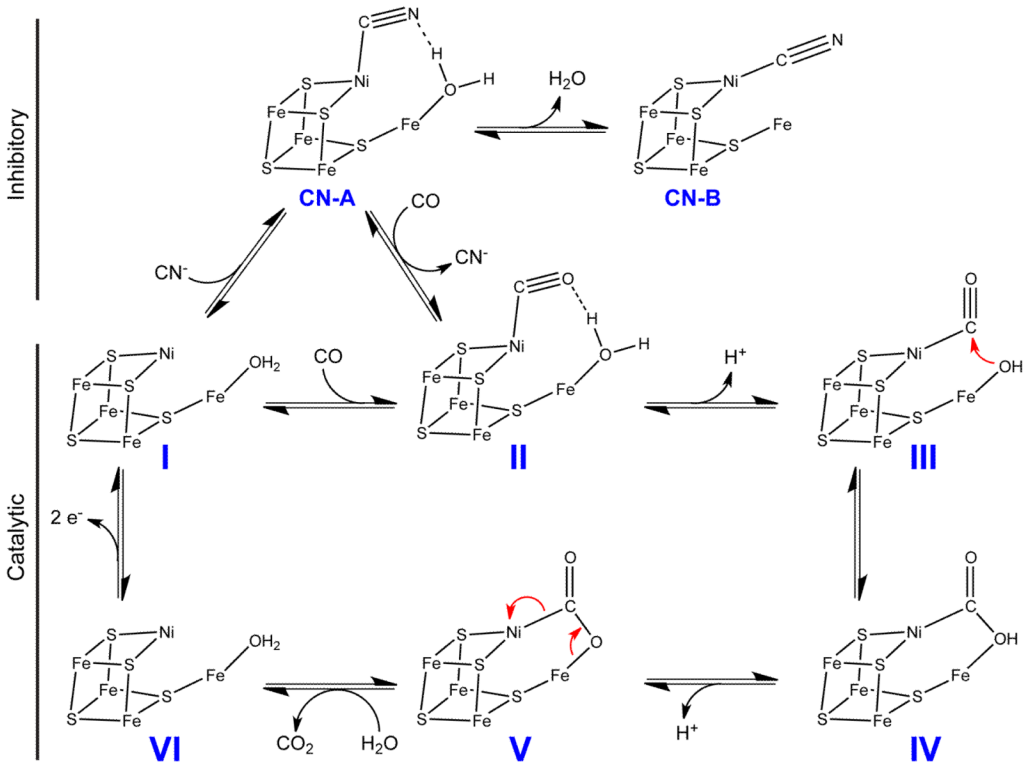

Figure 4.

Proposed catalytic and inhibitory mechanisms of the CODH C-cluster, consistent with crystal structures containing bound substrate and inhibitor molecules. To begin the reaction, a water molecule binds the unique Fe of the C-cluster (State I), as seen in *Ch*CODH and *Mt*CODH/ACS structures. CO binds Ni with bent geometry (State II), as seen in CO-bound *Mb*CODH and CN-bound *Mt*CODH/ACS. Upon deprotonation of water, a “carbon shift” may occur to position the carbon in close proximity to the resulting hydroxide (State III), promoting nucleophilic attack to yield a Ni-COOH intermediate (State IV). A second deprotonation gives a Ni-COO^{-} species (State V). The crystal structure of CO_2-bound *Ch*CODH resembles States IV and V, which differ only in protonation state. CO_2 may then be released, with the C-cluster becoming reduced by two electrons (State VI). Electrons are then passed to external electron acceptor proteins through a wire of [4Fe-4S] clusters within the CODH dimer, as seen in Figure 2A, completing the catalytic cycle. Protons generated during CO oxidation may access the external solvent through a histidine-lined channel. In the proposed inhibitory mechanism, cyanide competes with CO for binding to Ni of the C-cluster with bent geometry, as seen in the structure of cyanide-bound *Mt*CODH/ACS (State CN-A). Following displacement of Fe-bound water, cyanide may relax to a tighter linear binding mode, as seen in the structure of cyanide-bound *Ch*CODH (State CN-B).